SSSAJ

Soil Science Society of America Journal

Vol. 65 No. 4 July–August 2001 SSSJD4 65(4):1027–1350 (2001)

SOIL SCIENCE SOCIETY OF AMERICA JOURNAL

Business and Editorial Offices at
677 South Segoe Road, Madison, WI 53711
(www.soils.org)

Published bimonthly by the Soil Science Society of America, Inc. Periodicals postage paid at Madison, WI, and at additional mailing offices.

Postmaster: Send address change to *SSSA Journal*, 677 S. Segoe Rd., Madison, WI 53711.

Subscription rates (nonmember): $247 per year, within the USA; all others $271. Single copies, $30 USA; elsewhere, $36. Members are eligible for reduced subscription rates. New subscriptions, renewals, and new memberships that include the *SSSA Journal* begin with the first issue of the current year. Claims for copies lost in the mail must be received within 90 days of publication date for domestic subscribers, and within 26 weeks of publication date for foreign subscribers.

Membership in the Society is not a requirement for publication in *SSSA Journal*; however, nonmembers will be charged an additional amount for the first six published pages of a manuscript. To qualify for member rates, at least one author must be an active, emeritus, graduate student, or undergraduate student member of SSSA, CSSA, or ASA on the date the manuscript is accepted for publication.

Volunteered papers will be assessed a charge of $25 per page for nonmembers for each printed page from page one through page six; a charge of $190 per page ($95 per half page) will be assessed all papers for additional pages. No charge will be assessed against invited review papers or comments and letters to the editor. The Society absorbs the cost of reproducing illustrations up to $15 for each paper.

Contributions to the *SSSA Journal* may be (i) papers and notes on original research; and (ii) "Comments and Letters to the Editor" containing (*a*) critical comments on papers published in one of the Society outlets or elsewhere, (*b*) editorial comments by Society officers, or (*c*) personal comments on matters having to do with soil science. Letters to the Editor are limited to one printed page. Contributions need not have been presented at annual meetings. Original research findings are interpreted to mean the outcome of scholarly inquiry, investigation, or experimentation having as an objective the revision of existing concepts, the development of new concepts, or the improvement of techniques in some phase of soil science. Short, critical reviews or essays on timely subjects, upon invitation by the Editorial Board, may be published on a limited basis. Refer to SSSA Publication Policy (Soil Sci. Soc. Am. J. 64(1):1–3, 2000) and to the *Publications Handbook and Style Manual* (ASA-CSSA-SSSA, 1998).

Keep authors anonymous from reviewers by listing title, author(s), author–paper documentation, and acknowledgments on a detachable title page. Repeat manuscript title on the abstract page.

Manuscripts are to be sent to Dr. Lloyd R. Hossner, Editor, *SSSA Journal*, Soil and Crop Sciences Dep., Texas A&M University, College Station, TX 77843 (Phone: 979-845-3814). Four copies of the manuscript on line-numbered paper are required. All other correspondence should be directed to the Managing Editor, 677 S. Segoe Rd., Madison, WI 53711.

Trade names are sometimes listed in papers in this journal. No endorsement of these products by the publisher is intended, nor is any criticism implied of similar products not mentioned.

ISSN 0361-5995

IMPACTS OF EL NIÑO AND CLIMATE VARIABILITY ON AGRICULTURE

ASA Special Publication Number 63

NEW

El Niño impacts on agriculture, while typically negative, may be positive in some areas. Agricultural impacts are generally strongest in the Southern Hemisphere. In some large countries, such as Brazil and the USA, national crop yields reflect little El Niño influence, because opposite responses in different regions tend to cancel each other out.

In the USA, El Niño events often bring storms to the West Coast and rain to the South. Connections to the Midwest are generally weak, but studies have shown that during phases of the El Niño-La Niña cycle, the U.S. Corn Belt region experiences anomalies in precipitation and temperature patterns. These fluctuations affect crop development, which in turn affect yields. This special publication contains papers that evaluate the impacts of climate variability on crop production and the potential of using seasonal climate forecasts for enhancing agricultural production.

Impacts of El Niño and Climate Variability on Agriculture. Cynthia Rosenzweig, editor. Published by the American Society of Agronomy, Crop Science Society of America, and Soil Science Society of America. ASA Special Publication Number 63. Softcover, 126 pages, 2001. ISBN 0-89118-148-2. Price: $36.00 ($30.00 members first copy). **Item No. 40325.**

Please send me _____ copy(ies) of *Impacts of El Niño and Climate Variability on Agriculture*.

Method of payment: My Society Membership Number is _____

___ Check or U.S./international money order enclosed (Payable to: **American Society of Agronomy**)

___ Bill me ($2.00 invoicing charge)

___ Credit card (check one): ❑ Visa ❑ MasterCard ❑ Discover **A $2.00 processing fee will be added to credit card orders.**

Card Number _____ Expiration Date _____

Print Cardholder's Name _____

Name _____

Address _____

_____

City _____ State/Province _____ Zip/Postal Code _____ Country _____

All payments must be in U.S. funds drawn on a U.S. bank or add $40.00 U.S. to the total amount due. Advance payment and 10 percent per book for postage is required on all orders outside the United States. Wisconsin residents add appropriate sales tax. All overseas book orders are shipped surface mail unless airmail shipping costs have been paid in advance. Send your order to: ASA-CSSA-SSSA Headquarters Office; Attn: Book Order Department; 677 South Segoe Road; Madison, Wisconsin 53711-1086 USA.

Internet: http://www.agronomy.org **E-mail: books@agronomy.org** **FAX: 608-273-2021**

Methods of Soil Analysis

Number 5 in the Soil Science Society of America Book Series

Methods of Soil Analysis: Part 1—Physical and Mineralogical Methods

Great strides have been made in the conception of physical and mineralogical characteristics of soils and how they relate to each other and to chemical properties. The methods of analyses included here provide a uniform set of procedures which can be used by the majority of soil scientists and engineers. *A. Klute, ed. Hardcover, 1,188 pages, 1986; ASA and SSSA. Number 5 in the Soil Science Society of America Book Series. Nonmember Price: $60.00 ($52.00 if ordered with one of the other "Methods" books). Member Price: $50.00 ($43.00 if ordered with one of the other "Methods" books). ISBN 0-89118-811-8.*

Methods of Soil Analysis: Part 2—Microbiological and Biochemical Properties

Laboratories outside of soil science will find it advantageous to use the methods contained in this book. They will be particularly relevant and useful to laboratories with interest in environmental microbiology or bioremediation. Analytical methods are essential to progress in science and the methods presented in this book are recognized as being among the best currently available. *R.W. Weaver et al., ed. Hardcover, 1,121 pages, 1994; SSSA. Number 5 in the Soil Science Society of America Book Series. Nonmember Price: $65.00 ($56.00 if ordered with one of the other "Methods" books). Member Price: $55.00 ($47.00 if ordered with one of the other "Methods" books). ISBN 0-89118-810-X.*

Methods of Soil Analysis: Part 3—Chemical Methods

This volume covers newer methods for characterizing soil chemical properties as well as several methods for characterizing soil chemical processes. This book will serve as the primary reference on analytical methods. Updated chapters are included on the principles of various instrumental methods and their applications to soil analysis. New chapters are included on Fourier transform infrared, Raman, electron spin resonance, x-ray photoelectron, and x-ray absorption fine structure spectroscopies. *D.L. Sparks et al., ed. Hardcover, 1,358 pages, 1996; SSSA and ASA. Number 5 in the Soil Science Society of America Book Series. Nonmember Price: $65.00 ($56.00 if ordered with one of the other "Methods" books). Member Price: $55.00 ($47.00 if ordered with one of the other "Methods" books). ISBN 0-89118-825-8.*

Note: When ordering **Methods of Soil Analysis**, please include the editor(s) name(s) in your order. This will allow for smoother processing of your order.

I would like to order the following publications:

_____ *Methods of Soil Analysis: Part 1—Physical and Mineralogical Methods*
_____ *Methods of Soil Analysis: Part 2—Microbiological and Biochemical Properties*
_____ *Methods of Soil Analysis: Part 3—Chemical Methods*

My Society Membership Number is _____

Method of payment:

___ Check or U.S./international money order enclosed (Payable to: **American Society of Agronomy**)
___ Bill me ($2.00 invoicing charge)
___ Credit card (check one): ❑ Visa ❑ MasterCard ❑ Discover
A $2.00 processing fee will be added to credit card orders.

Card Number _____ Expiration Date _____

Print Cardholder's Name _____

Name _____

Address _____

_____

City _____ State/Province _____ Zip/Postal Code _____ Country _____

All payments must be in U.S. funds drawn on a U.S. bank or add $40.00 U.S. to the total amount due. Advance payment and 10 percent per book for postage is required on all orders outside the United States. Wisconsin residents add appropriate sales tax. All overseas book orders are shipped surface mail unless airmail shipping costs have been paid in advance. Send your order to: SSSA, ASA Headquarters Office; Attn: Book Order Department; 677 South Segoe Road; Madison, Wisconsin 53711-1086 USA.

FAX: 608-273-2021 **INTERNET: http://www.agronomy.org/pubcat/**

Conversion Factors for SI and non-SI Units

To convert Column 1 into Column 2, multiply by	Column 1 SI Unit	Column 2 non-SI Unit	To convert Column 2 into Column 1, multiply by
	Length		
0.621	kilometer, km (10^3 m)	mile, mi	1.609
1.094	meter, m	yard, yd	0.914
3.28	meter, m	foot, ft	0.304
1.0	micrometer, μm (10^{-6} m)	micron, μ	1.0
3.94×10^{-2}	millimeter, mm (10^{-3} m)	inch, in	25.4
10	nanometer, nm (10^{-9} m)	Angstrom, Å	0.1
	Area		
2.47	hectare, ha	acre	0.405
247	square kilometer, km^2 (10^3 m)^2	acre	4.05×10^{-3}
0.386	square kilometer, km^2 (10^3 m)^2	square mile, mi^2	2.590
2.47×10^{-4}	square meter, m^2	acre	4.05×10^3
10.76	square meter, m^2	square foot, ft^2	9.29×10^{-2}
1.55×10^{-3}	square millimeter, mm^2 (10^{-3} m)^2	square inch, in^2	645
	Volume		
9.73×10^{-3}	cubic meter, m^3	acre-inch	102.8
35.3	cubic meter, m^3	cubic foot, ft^3	2.83×10^{-2}
6.10×10^4	cubic meter, m^3	cubic inch, in^3	1.64×10^{-5}
2.84×10^{-2}	liter, L (10^{-3} m^3)	bushel, bu	35.24
1.057	liter, L (10^{-3} m^3)	quart (liquid), qt	0.946
3.53×10^{-2}	liter, L (10^{-3} m^3)	cubic foot, ft^3	28.3
0.265	liter, L (10^{-3} m^3)	gallon	3.78
33.78	liter, L (10^{-3} m^3)	ounce (fluid), oz	2.96×10^{-2}
2.11	liter, L (10^{-3} m^3)	pint (fluid), pt	0.473
	Mass		
2.20×10^{-3}	gram, g (10^{-3} kg)	pound, lb	454
3.52×10^{-2}	gram, g (10^{-3} kg)	ounce (avdp), oz	28.4
2.205	kilogram, kg	pound, lb	0.454
0.01	kilogram, kg	quintal (metric), q	100
1.10×10^{-3}	kilogram, kg	ton (2000 lb), ton	907
1.102	megagram, Mg (tonne)	ton (U.S.), ton	0.907
1.102	tonne, t	ton (U.S.), ton	0.907
	Yield and Rate		
0.893	kilogram per hectare, kg ha^{-1}	pound per acre, lb acre^{-1}	1.12
7.77×10^{-2}	kilogram per cubic meter, kg m^{-3}	pound per bushel, bu^{-1}	12.87
1.49×10^{-2}	kilogram per hectare, kg ha^{-1}	bushel per acre, 60 lb	67.19
1.59×10^{-2}	kilogram per hectare, kg ha^{-1}	bushel per acre, 56 lb	62.71
1.86×10^{-2}	kilogram per hectare, kg ha^{-1}	bushel per acre, 48 lb	53.75
0.107	liter per hectare, L ha^{-1}	gallon per acre	9.35
893	tonnes per hectare, t ha^{-1}	pound per acre, lb acre^{-1}	1.12×10^{-3}
893	megagram per hectare, Mg ha^{-1}	pound per acre, lb acre^{-1}	1.12×10^{-3}
0.446	megagram per hectare, Mg ha^{-1}	ton (2000 lb) per acre, ton acre^{-1}	2.24
2.24	meter per second, m s^{-1}	mile per hour	0.447
	Specific Surface		
10	square meter per kilogram, m^2 kg^{-1}	square centimeter per gram, cm^2 g^{-1}	0.1
1000	square meter per kilogram, m^2 kg^{-1}	square millimeter per gram, mm^2 g^{-1}	0.001
	Pressure		
9.90	megapascal, MPa (10^6 Pa)	atmosphere	0.101
10	megapascal, MPa (10^6 Pa)	bar	0.1
1.00	megagram per cubic meter, Mg m^{-3}	gram per cubic centimeter, g cm^{-3}	1.00
2.09×10^{-2}	pascal, Pa	pound per square foot, lb ft^{-2}	47.9
1.45×10^{-4}	pascal, Pa	pound per square inch, lb in^{-2}	6.90×10^3

(continued on next page)

Conversion Factors for SI and non-SI Units

To convert Column 1 into Column 2, multiply by	Column 1 SI Unit	Column 2 non-SI Unit	To convert Column 2 into Column 1, multiply by
	Temperature		
1.00 (K − 273)	Kelvin, K	Celsius, °C	1.00 (°C + 273)
(9/5 °C) + 32	Celsius, °C	Fahrenheit, °F	5/9 (°F − 32)
	Energy, Work, Quantity of Heat		
9.52×10^{-4}	joule, J	British thermal unit, Btu	1.05×10^{3}
0.239	joule, J	calorie, cal	4.19
10^{7}	joule, J	erg	10^{-7}
0.735	joule, J	foot-pound	1.36
2.387×10^{-5}	joule per square meter, J m^{-2}	calorie per square centimeter (langley)	4.19×10^{4}
10^{5}	newton, N	dyne	10^{-5}
1.43×10^{-3}	watt per square meter, W m^{-2}	calorie per square centimeter minute (irradiance), cal cm^{-2} min^{-1}	698
	Transpiration and Photosynthesis		
3.60×10^{-2}	milligram per square meter second, mg m^{-2} s^{-1}	gram per square decimeter hour, g dm^{-2} h^{-1}	27.8
5.56×10^{-3}	milligram (H_2O) per square meter second, mg m^{-2} s^{-1}	micromole (H_2O) per square centimeter second, μmol cm^{-2} s^{-1}	180
10^{-4}	milligram per square meter second, mg m^{-2} s^{-1}	milligram per square centimeter second, mg cm^{-2} s^{-1}	10^{4}
35.97	milligram per square meter second, mg m^{-2} s^{-1}	milligram per square decimeter hour, mg dm^{-2} h^{-1}	2.78×10^{-2}
	Plane Angle		
57.3	radian, rad	degrees (angle), °	1.75×10^{-2}
	Electrical Conductivity, Electricity, and Magnetism		
10	siemen per meter, S m^{-1}	millimho per centimeter, mmho cm^{-1}	0.1
10^{4}	tesla, T	gauss, G	10^{-4}
	Water Measurement		
9.73×10^{-3}	cubic meter, m^3	acre-inches, acre-in	102.8
9.81×10^{-3}	cubic meter per hour, m^3 h^{-1}	cubic feet per second, ft^3 s^{-1}	101.9
4.40	cubic meter per hour, m^3 h^{-1}	U.S. gallons per minute, gal min^{-1}	0.227
8.11	hectare-meters, ha-m	acre-feet, acre-ft	0.123
97.28	hectare-meters, ha-m	acre-inches, acre-in	1.03×10^{-2}
8.1×10^{-2}	hectare-centimeters, ha-cm	acre-feet, acre-ft	12.33
	Concentrations		
1	centimole per kilogram, cmol kg^{-1}	milliequivalents per 100 grams, meq 100 g^{-1}	1
0.1	gram per kilogram, g kg^{-1}	percent, %	10
1	milligram per kilogram, mg kg^{-1}	parts per million, ppm	1
	Radioactivity		
2.7×10^{-11}	becquerel, Bq	curie, Ci	3.7×10^{10}
2.7×10^{-2}	becquerel per kilogram, Bq kg^{-1}	picocurie per gram, pCi g^{-1}	37
100	gray, Gy (absorbed dose)	rad, rd	0.01
100	sievert, Sv (equivalent dose)	rem (roentgen equivalent man)	0.01
	Plant Nutrient Conversion		
	Elemental	***Oxide***	
2.29	P	P_2O_5	0.437
1.20	K	K_2O	0.830
1.39	Ca	CaO	0.715
1.66	Mg	MgO	0.602

Suggestions for Contributors to the *Soil Science Society of America Journal*

General Requirements

Contributions to the *SSSA Journal* may be (i) papers and notes on original research; and (ii) "Comments and Letters to the Editor" containing (*a*) critical comments on papers published in one of the Society outlets or elsewhere, (*b*) editorial comment or comments by Society officers, or (*c*) personal comments on matters having to do with soil science. Notes are not to exceed two printed pages; Letters to the Editor, one printed page. Contributions need not have been presented at annual meetings. Original research findings are interpreted to mean the outcome of scholarly inquiry, investigation, modeling, or experimentation having as an objective the revision of existing concepts, the development of new concepts, or the development of new or improved techniques in some phase of soil science. Authors are encouraged to test modeling results with measurements or published data. Short, critical reviews or essays on timely subjects, upon invitation by the Editorial Board, may be published on a limited basis. See SSSA Publication Policy (Soil Sci. Soc. Am. J. 63:1–3, 1999).

Membership in the Society is not a requirement for publication in the *SSSA Journal*; however, nonmembers will be charged for the first six published pages of a manuscript. To qualify for member rates, at least one author must be an active, emeritus, graduate student, or undergraduate student member of SSSA, CSSA, or ASA on the date the manuscript is accepted for publication.

The *Publications Handbook and Style Manual* (1998) is the official guide for the preparation and editing of papers. Copies are available from the ASA Headquarters, 677 S. Segoe Rd., Madison, WI 53711.

Manuscripts

COPIES—Submit four legible double-spaced copies of each manuscript on 21.6- by 27.9-cm paper. The lines of type must be numbered on each page, and at least 2.5-cm margins left on top, bottom, and sides. Pages should be numbered consecutively. Type legends for figures (double spaced) on one or more sheets and place at the end of the manuscipt.

A cover letter should accompany each submission and should include suggestions of potential reviewers. These reviewers must not have a conflict of interest involving the authors or paper and the editorial board has the right to not use any reviewers suggested by authors.

TITLE—A short title, not exceeding 12 words, is required. It must accurately identify and describe the manuscript contents.

AUTHOR–PAPER DOCUMENTATION—Include this at the bottom of the title page. It should include all authors' names and complete mailing addresses, sponsoring organization, and date received. Use an asterisk in the author byline to identify the corresponding author. Professional titles are not listed. Other information, such as grant funding, may be included here or placed in an acknowledgment, also on the title page. To ensure an unbiased review, the title page will be removed during the review process. The title, but not the byline, should therefore be repeated on the page that contains the abstract.

TEXT FOOTNOTES—Supplementary notes, such as a disclaimer on a commericial product, are numbered consecutively starting with no. 1 and should be typed at the bottom of the text page concerned.

ABSTRACT—An informative, self-explanatory abstract, not exceeding 250 words (150 words for notes), must be supplied on a separate page. It should specifically tell why and how the study was made, what the results were, and why they were important. Use quantitative terms. The title should be repeated on top of the abstract page without author identification.

TABLES—Each table must be on a separate sheet and numbered consecutively. Do not duplicate matter presented in charts or graphs. Use the following symbols for footnotes in the order shown: †, .., ■, ¶, #, ††, ..., etc.

The symbols *, **, and *** are used to show statistical significance at 0.05, 0.01, and 0.001 levels, respecitvely, and are not used for other footnotes.

FIGURES—Do not use figures that duplicate matter in tables. Photographs for halftone reproduction should be glossy prints with good dark and light contrast. Prepare drawings for graphs and charts with India ink on white drawing paper or tracing vellum. Typewritten matter is not acceptable. Sharp photocopies and laser-printed originals are acceptable if free of distortion.

If possible, use photographs and drawings that can be reduced to 1-column width (8.5 cm or 20 picas). A good size for a drawing is twice that desired in the printed figure. It is not desirable to have capital letters or numbers in the printed illustration smaller than 1.75 mm; lowercase letters or symbols should be not less than 1.25 mm high. Label each figure with title of article and figure number. Machine photocopies of charts and graphs, with captions attached, are preferred in the review process.

Manuscripts, four complete copies, should be submitted in double blind format (see Abstract and Acknowledgment) to the Editor:

Dr. Lloyd R. Hossner
Editor, SSSA Journal
Soil and Crop Sciences Department
Texas A&M University
College Station, TX 77843 Phone: 409-845-3814

REFERENCES—The author–year system is preferred, but the number reference system will be accepted. If you use the author–year system, do not number the reference list. Citations should include names of all authors, year of publication, complete title, publication or journal title, volume number, and inclusive pages. Keep in mind the following:

1. Arrange the list alphabetically by the names of the first authors and then by the second and third authors.
2. Single-authored articles should precede multiple-author articles for which the individual is senior author.
3. Two or more articles by the same author(s) are listed chronologically; two or more in the same year are indicated by the letters a, b, c, etc.
4. All published works referred to in the text must be listed.
5. Only literature that is available through libraries can be cited. The reference list can include theses, dissertations, and abstract publications.
6. Material not available through libraries, such as personal communications or privileged data, should be cited in the text in parenthetical form.
7. Chapter references from books must include author(s), year, chapter, title, pages, editor(s), book title, publisher, and city.
8. Symposium proceedings should include editor, date and place of symposium, publisher, and page numbers.

ACKNOWLEDGMENTS—These should be on a separate page following the title page. The title page and acknowledgments will not be provided to reviewers so that authors remain anonymous.

REVISION OF MANUSCRIPTS—Authors have four months to revise and return their manuscript following reviewer and associate editor comments. If not returned within four months, the manuscript will be released; it must then be resubmitted as a new paper.

Style Guidelines

Both the accepted common name and the chemical name of pesticides must be given when first mentioned in the abstract or text. Similarly, the Latin binomial or trinomial and authority must be shown for all plants, insects, pathogens, and animals at first listing in the abstract or main text.

SI units must be used in all manuscripts (see *Publications Handbook and Style Manual*, 1988). Corresponding units may be added in parentheses at the discretion of the author.

Length of Manuscript and Page Charges

Volunteered papers will be assessed a page charge of $25 per printed page for nonmembers for each page from page one through page six; production charges of $190 per page ($95 per half page) will be assessed for additional pages for all papers. No page charges will be assessed against invited review papers, Comments, or Letters to the Editor.

In general, four manuscript pages will equal one printed page. For space economy, Materials and Methods, long Literature Reviews, theory, soil or site descriptions, etc., footnotes, tables, figure captions, and references are set in small type. Each table and figure will usually take 1/4 of a printed page.

For tabular matter, 9 lines of typewritten matter equal 1 column-inch of type. Allow also for rules and spacing. Tables with more than 35 units (including space between words) in a horizontal line can rarely be set 1 page-column wide.

The depth of a printed figure will be in the same proportion to the width (1 column = 8.4 cm; 2 column = 17.8 cm) as that of the corresponding dimensions in the original drawing.

July 2000

SSSAJ July–August 2001 Vol. 65, No. 4

Soil Science Society of America Journal

Continued on page iv

This issue's cover: The dominant soils of the Abitibi region in Northwestern Quebec have evolved on clay-rich sediments deposited by postglacial Lake Barlow-Ojibway. They are characterized by a highly porous E horizon (top right) and a contrasting, more massive Bt (top left) or Btg (bottom) horizon. These soils support very productive stands of boreal species. Maintaining their productive capacity represents one of the challenges of sustainable forest management in this region. See "Persistence of Soil Compaction and Effects on Seedling Growth in Northwestern Quebec" by Suzanne Brais, p. 1263–1271. (Photo by Jacques Brisson.)

Continued from page iii

SOIL SCIENCE SOCIETY OF AMERICA
JOURNAL

VOL. 65 JULY–AUGUST 2001 No. 4

DIVISION S-1—SOIL PHYSICS

Calibration of a Two-Dimensional Root Water Uptake Model

J. A. Vrugt, J. W. Hopmans,* and J. Šimunek

ABSTRACT

Although solutions of multidimensional transient water flow can be obtained by numerical modeling, their application may be limited in part as root water uptake is generally considered to be one-dimensional only. The objective of this study was to develop and test a two-dimensional root water uptake model, which can be incorporated into numerical multidimensional flow models. The two-dimensional uptake model is based on the model by Raats, but is extended with a radial component. Subsequently, the root water uptake model was incorporated into a two-dimensional flow model, and root water uptake parameters were optimized, minimizing the residuals between measured and simulated water content data. Water content was measured around a sprinkler-irrigated almond tree (*Prunus laurocerasus* M.J.Roem) for a 16-d period at 25 locations, following irrigation. To calibrate the flow and root water uptake model, a genetic algorithm (GA) was used to find the approximate global minimum of the optimized parameter space. The final fitting parameters were determined using the Simplex algorithm (SA). With the optimized root water uptake parameters, simulated and measured water contents during the 16-d period were in excellent agreement, with R^2 values generally ranging between 0.94 and 0.99 and a root mean squared error (RMSE) of 0.015 $m^3 m^{-3}$. The developed root water uptake model is extremely flexible and allows spatial variations of water uptake as influenced by nonuniform (drip irrigation) and uniform water application patterns.

FROM A HYDROLOGICAL PERSPECTIVE, water uptake by root systems and their spatial distribution can largely control water fluxes to the atmosphere and the groundwater (Canadell et al., 1996). For an improved understanding of the magnitude of these fluxes, accurate estimates of the temporal and spatial root water uptake patterns are needed. Quantification of root water extraction rates also contributes to an improved understanding of chemical fluxes in the vadose zone in both ecological and hydrological studies (Somma et al., 1998), as well as their control by vegetation. Water uptake by rooting systems can control the timing and the amount of chemical pollutant loadings to the groundwater through elimination of preferential flow patterns of water and chemicals, or by regulation of absorption of nutrients or trace elements, thereby reducing their concentration levels in the deep vadose zone or groundwater (Clothier and Green, 1994). Moreover, the rhizosphere might be responsible for accelerated breakdown of organic chemicals by biodegradation (Walton and Anderson, 1990).

Actual root water uptake not only depends on the root distribution and its functioning, but also on soil water availability and salinity. In addition to water stress in periods of low water availability, root water uptake is also reduced when concentrations of soluble salts exceed plant-specific threshold values (Homaee, 1999). In irrigated soils, particularly in arid and semiarid regions, plants are generally subjected to both salinity and water stress. In these regions, soil and water management practices are based on maintaining a favorable soil water content and salinity status in the root zone, thereby minimizing periods of water stress while controlling leaching to minimize salinity stress.

The influence of plant–root systems on water and chemical movement can be better understood using soil water simulation models, provided that accurate spatial and temporal root water uptake distributions are included (Musters and Bouten, 1999; Musters, 1998). The

J.A. Vrugt, Institute for Biodiversity and Ecosystem Dynamics, University of Amsterdam, The Netherlands, Nieuwe Prinsengracht 130, Amsterdam, 1018 VZ; J.W. Hopmans, Hydrology Program, Dept. Land, Air and Water Resources (LAWR), University of California, Davis, CA 95616, USA; J. Šimunek, USDA Salinity Laboratory, University of California, Riverside, CA 95207, USA. Received 18 Nov. 1999 *Corresponding author (jwhopmans@ucdavis.edu).

Published in Soil Sci. Soc. Am. J. 65:1027–1037 (2001).

Abbreviations: CIMIS, California Irrigation Management Information System; CV, coefficient of variation; GA, genetic algorithm; RMSE, root mean squared error; SA, simplex algorithm.

most common approach for modeling root water uptake in unsaturated flow is based on introducing a sink term, S, in the Richards equation (Whisler et al., 1968; Molz, 1981; Clausnitzer and Hopmans, 1994) describing transient multidimensional water flow:

$$\frac{\partial \theta}{\partial t} = \nabla[K\nabla(h - z)] - S \qquad [1]$$

where θ is the volumetric water content ($L^3\ L^{-3}$); K is the unsaturated hydraulic conductivity ($L\ T^{-1}$); h (L) is the soil water pressure head; z (positive downwards) denotes the gravitational head (L) (to be included for the vertical flow component only); and S is the volumetric sink term ($L^3\ L^{-3}\ T^{-1}$), being a function of both space and time. However, application of multidimensional flow models requires the spatial characterization of root water uptake as well. Available uptake models are largely limited to one dimension only (Feddes et al., 1974; Molz, 1981; Jarvis, 1989), describing variations in water uptake with soil depth while allowing for reduction in uptake by soil water stress. Exceptions are the two-dimensional models proposed by Neuman et al. (1975) and Warrick et al. (1980). However, their application to describe different types of root distributions is fairly limited. Most recently, Coelho and Or (1996) proposed bivariate gaussian root distribution density functions (normal, semilognormal and lognormal) as parametric models for the description of root water uptake patterns of drip-irrigated row crops.

It is the objective of this study to develop a flexible multidimensional root water uptake model to be integrated in the two-dimensional HYDRUS-2D flow code (Šimunek et al., 1999). Furthermore, the root water model was calibrated using the spatial distribution of water contents around a sprinkler-irrigated almond tree during a 16-d monitoring period.

MATERIALS AND METHODS

Root Water Uptake Model

As basis of the proposed root water uptake model, we used the exponential model by Raats (1974),

$$\beta(z) = \frac{1}{\lambda} e^{-\frac{z}{\lambda}} \qquad [2]$$

where $\beta(z)$ is the spatial root water uptake distribution with depth (L^{-1}); λ (L) is selected such that at depth λ the cumulative root water uptake is 63% of total uptake over the whole root zone; and z is the depth in the soil profile ($z \geq 0$). The proposed model excludes λ, but includes three additional parameters

$$\beta(z) = \left[1 - \frac{z}{z_m}\right] e^{-\frac{p_z}{z_m}|z^* - z|}; \qquad z \geq 0 \qquad [3]$$

where $\beta(z)$ denotes the dimensionless spatial root distribution with depth; z_m is the maximum rooting depth (L); and p_z (-) and z^* (L) are empirical parameters. These parameters were included to provide for zero root water uptake at $z \geq z_m$, to account for nonsymmetrical root water uptake with depth and to allow for maximum root water uptake at any depth, z^{max} ($0 \leq z^{max} \leq z_m$). The nonsymmetry in root water uptake with soil depth is determined by the ratio between p_z for $z \leq z^*$, and the p_z value for $z > z^*$. To reduce the number of parameters, p_z is set to unity for values of $z > z^*$, whereas it is a fitted value for $z \leq z^*$. The value of $z = z^{max}$ can be calculated from the first derivative, i.e., $d\beta/dz = 0$.

As the potential cumulative root water uptake must equal the potential transpiration rate (T_{pot}), the normalized root water uptake distribution, S_m (T^{-1}), with depth is computed

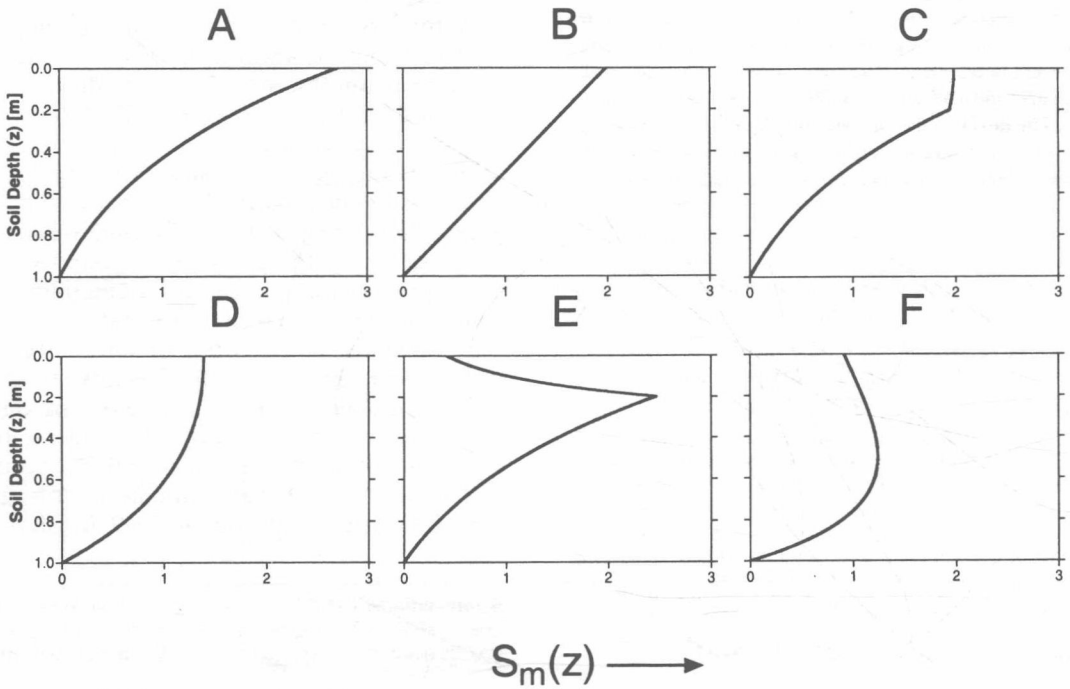

Fig. 1. Representation of different root water uptake models, $S_m(z)$, with depth.

from

$$S_m(z) = \frac{\beta(z)T_{pot}}{\int_{z=z_m}^{z=0} \beta(z)dz} \quad [4]$$

Since in most field studies, z_m is known a priori, the uptake model of Eq. [3] contains only two unknown parameters (p_z and z^*). Figure 1 shows six different possible configurations of normalized root water uptake distribution, using z_m equals 1.0 m. The corresponding parameter values for the different models are listed in Table 1. The first four root water uptake models (A, B, C, and D) have maximum root water uptake at the soil surface ($z_{max} = 0$), whereas the other two uptake distributions (E and F) simulate maximum uptake at z_{max} values of 0.2 and 0.5 m, respectively, as may be caused by subsurface drip irrigation.

For the characterization of the uptake intensity along the radial direction we used a similar expression as Eq. [3];

$$\beta(r) = \left[1 - \frac{r}{r_m}\right] e^{-\frac{p_r}{r_m}|r^* - r|}; \qquad r \geq 0 \quad [5]$$

where $\beta(r)$ characterizes the dimensionless spatial distribution of unstressed root water uptake in the r direction; r_m is the maximum rooting length in the radial direction (L); r is the radial distance from the origin of the plant (L) and p_r and r^* are empirical parameters with units (-) and (L), respectively. As in Eq. [3] we set p_r to unity for $r > r^*$.

Combining the uptake intensity along the z-direction (Eq. [3]) with the uptake intensity along the radial direction leads to a two-dimensional root water uptake model, which can be expressed as

$$\beta(r,z) = \left[\left(1 - \frac{z}{z_m}\right)\right]\left[\left(1 - \frac{r}{r_m}\right)\right] e^{-\left(\frac{p_z}{z_m}|z^* - z| + \frac{p_r}{r_m}|r^* - r|\right)} \quad [6]$$

where $\beta(r,z)$ denotes the dimensionless two-dimensional spatial distribution of root water uptake.

Both the presented water uptake model and the bivariate gaussian density functions presented by Coelho and Or (1996) contain six parameters. However, the proposed model includes at least two parameters (z_m and r_m) with a physical meaning. In contrast to the model of Coelho and Or (1996), Eq. [6] can be directly evaluated in the limit as $z \rightarrow 0$ and $r \rightarrow 0$. The single expression of Eq. [6] can simulate a wide variety of root water uptake patterns, whereas Coelho and Or (1996) introduce different distribution functions that need to be evaluated between uptake patterns.

Denoting the normalized root water uptake, S_m, as the vol-

Table 1. Parameter values for different water uptake distributions under nonstress conditions.

Model	Literature (adapted from)	z^*	p_z
		m	-
A	Raats, 1974	0.00	-†
B	Prasad, 1988	1.00	0.01
C	Hoffman and van Genuchten, 1983	0.20	1.00
D		0.20	10.0
E		1.00	1.00
F		1.00	2.00

† Model does not include parameter similar to p_z.

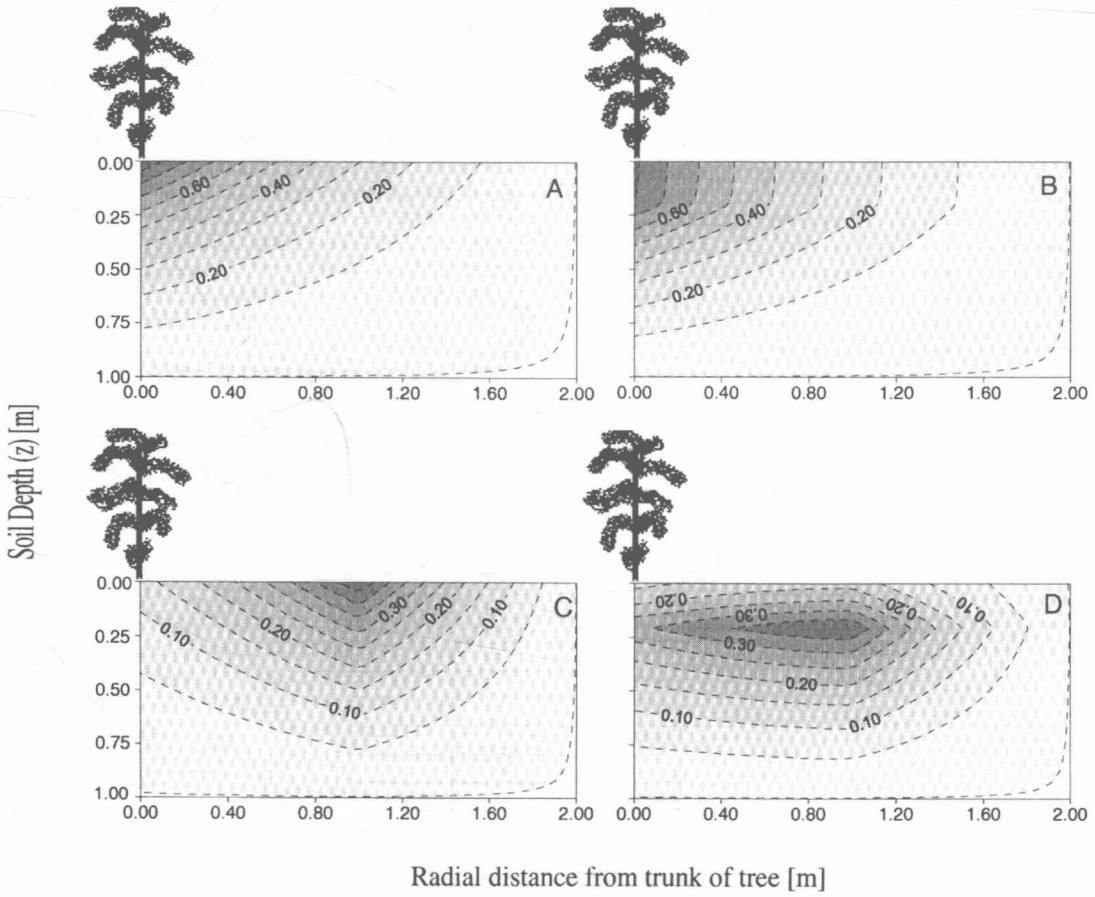

Fig. 2. Four different configurations of two-dimensional spatial distribution of potential root water uptake, $\beta(r,z)$.

Table 2. Parameter values for the two-dimensional root water uptake configurations in Fig. 2.

Figure	fitting parameters						derived	
	z_m	r_m	z^*	r^*	p_z	p_r	z^{max}	r^{max}
	m				(-)			
A	1.00	2.00	0.00	0.00	1.00	1.00	0.00	0.00
B	1.00	2.00	0.20	0.00	1.00	1.00	0.20	0.00
C	1.00	2.00	0.00	1.00	1.00	4.00	0.00	1.00
D	1.00	2.00	0.20	1.00	5.00	2.00	0.20	1.00

ume of water extracted per unit time and volume of soil while assuming axial symmetry, it follows that (Šimunek et al., 1999)

$$S_m(r,z) = \frac{\pi R^2 \beta(r,z)\, T_{pot}}{2\pi \int_0^{z_m} \int_0^{r_m} r\beta(r,z)\,dr\,dz} \quad [7]$$

where $S_m(r,z)$ denotes the normalized root water uptake rate (T^{-1}) and R is the size of the flow domain in the r-direction. If $r_m < R$ then the value of R in Eq. [7] automatically equals r_m.

Four different types of two-dimensional root water uptake patterns for unstressed conditions are presented in Fig. 2, which were simulated with the proposed model in Eq. [6]. The corresponding parameters of the different water uptake distributions are listed in Table 2. A root water uptake intensity pattern as presented in Fig. 2a,b is expected for uniform water application. Much different uptake patterns are shown in Fig. 2c (surface irrigation) and Fig. 2d (subsurface irrigation), where the location of maximum uptake intensity shifts to locations with maximum irrigation application rate for nonuniform water applications. The proposed root water uptake model can be easily extended to three dimensions by including an additional exponential term in Eq. [6]. Moreover, the model can be adapted to account for root growth by allowing time-dependent z_m and r_m values during a growing season.

To provide for root water uptake under water-stressed conditions, a soil water stress response function was included (van Genuchten, 1987).

$$\gamma(r,z,h) = \frac{1}{\left[1 + \left(\frac{h}{h_{50}}\right)^p\right]} \quad [8]$$

where h is the soil water pressure head at spatial location (r, z); h_{50} is the soil water pressure head (L) at which root water uptake rate is reduced by 50%; and p is a fitting parameter (-). The parameter p is usually assumed to be 3 (van Genuchten and Gupta, 1993).

Finally, the actual root water uptake rate at (r,z) can be calculated from

$$S(h,r,z) = \gamma(r,z,h) S_m(r,z) \quad [9a]$$

and

$$T_{pot} = K_c ET_0 - E_s \quad [9b]$$

where $S(h,r,z)$ is the actual water uptake (T^{-1}); K_c is the crop coefficient (-); ET_0 is the reference evapotranspiration (LT^{-1}); and E_s denotes soil evaporation (LT^{-1}). Hence, the actual transpiration rate (T_a) can be computed from Eq. [10].

$$T_a = \frac{2\pi}{\pi R^2} \int_0^{z_m} \int_0^{r_m} rS(h,r,z)\,dr\,dz \quad [10]$$

Field Description and Measurements

The experimental plot is located in an almond orchard, and covers about one quarter of the wetted area of a microsprinkler irrigating a single almond tree (Koumanov et al., 1997). In the 2.0 m by 2.0 m instrumented area, 25 polyvinyl chloride neutron probe access tubes were installed in a square grid of 0.50 m spacing to a depth of 90 cm (Fig. 3). The neutron probe was calibrated from gravimetric measurements using soil samples collected at soil depths of 15, 30, 45, 60, 75, and 90 cm during and after access tube installation. Separate calibration curves were used for the 0- to 15-cm surface soil and the 30- to 90-cm soil depth interval. Standard errors of estimate of volumetric water content curves were approximately 0.01 (15 cm depth interval) and 0.02 $m^3\ m^{-3}$ (all other measurements

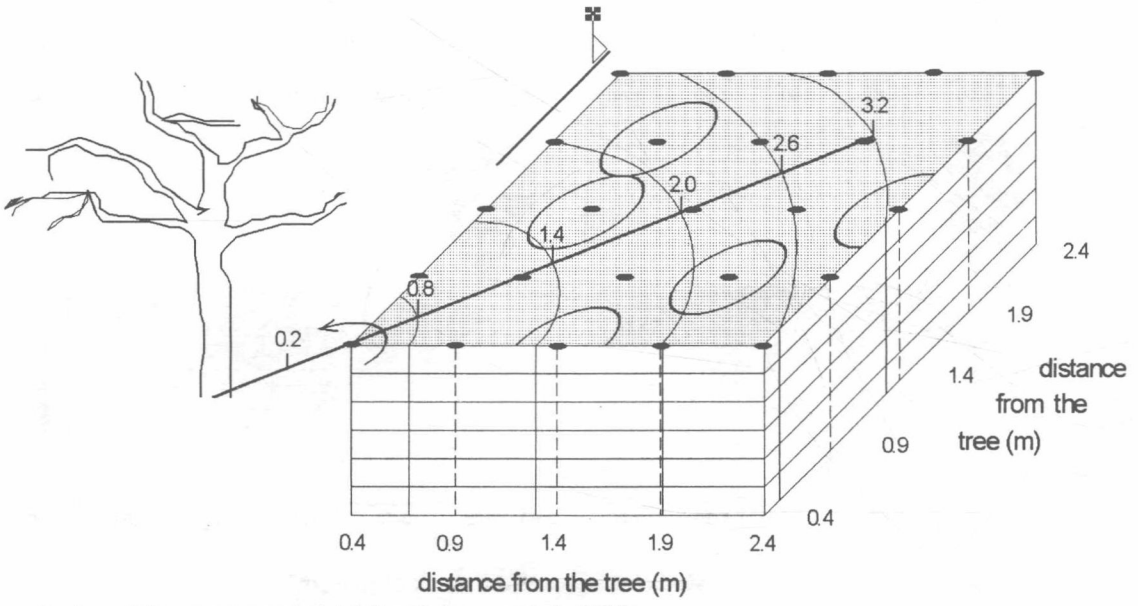

Fig. 3. Schematic view of the experimental plot (after Koumanov et al., 1997).

depths). The field is slightly undulating, and the soil is a shallow gravely loam (Andreu et al., 1997), overlaying a sloping high density restricting clay layer at about the 90- to 120-cm soil depth. The study by Andreu et al. (1997) indicated that root water uptake during the growing season was mainly limited to the top 60 cm, and that drainage of the soil primarily occurred by lateral flow along the sloping restricting clay layer.

The measurements were carried out 13 September through 29 September in the summer of 1995. First, the sprinkler system was used to moisten the whole soil profile. Neutron probe measurements were taken on 13 September, immediately after the irrigation at 1300, 1500, and 1800 h, during the period of 14 Septenber through 17 September, every 4 h at 600, 1000, 1400, and 1800 h, and during the period of 18 September through 29 September, daily at ~1000 h.

To simplify testing of the root water uptake model, the three dimensional grid measurements of water content needed to be reduced to two dimensions (r and z). For this we assumed that (i) the root water uptake around the tree was axisymmetrical and (ii) that the measurement volume of the neutron probe water content was a sphere with a constant radius of ~0.25 m. Although the first assumption was rather arbitrary, there was no reason to expect the contrary.

First, for each depth interval the rectangular measurement grid of Fig. 3 was partitioned into five concentric adjacent 0.6-m wide circular strips with the origin of the circles defining these soil strips. The soil strips were determined by the neutron access pipe location closest to the tree trunk (see Fig. 3). Second, a radial-average water content value was computed for each of the five soil areas (0.2–0.8, 0.8–1.4, 1.4–2.0, 2.0–2.6, and 2.6–3.2 m) using weighting factors for each neutron probe location with values equal to the fraction of the measurement volume fitting within the respective concentric soil area. We used 0.6 m wide strips for each of the five soil areas to ensure that enough water content measurements were contained within the respective strip. Moreover, the averaging using the 0.6-m wide strips gave the best agreement in total water depletion of the reduced two-dimensional domain as compared to the original three-dimensional grid of water content measurements. Since the averaging procedure was applied to depth intervals of 0 to 0.15, 0.15 to 0.3, 0.3 to 0.45, and 0.45 to 0.6, the final two-dimensional map included 20 average water content values at each measurement time (four depth intervals and five radial distance increments) during the 13 September to 29 September calibration period.

Water Flow Simulation

While assuming axial symmetry for an isotropic soil, the Richards equation for a rigid porous media can be written as (Inoue et al., 1998; Šimunek et al., 1999)

$$C\frac{\partial h}{\partial t} = \frac{1}{r}\frac{\partial}{\partial r}\left(rK\frac{\partial h}{\partial r}\right) + \frac{\partial}{\partial z}\left(K\frac{\partial h}{\partial z}\right) - \frac{\partial K}{\partial z} - S(h,r,z) \qquad [11]$$

where C is the water capacity (L^{-1}); h is the soil water pressure head (L); r is the radial coordinate; z is the vertical coordinate (positive downwards); t is time (T); and $S(h,r,z)$ denotes root water uptake (T^{-1}). Equation [11] was solved with the HYDRUS–2D model (Šimunek et al., 1999) using the Galerkin finite element method based on the mass conservative iterative scheme proposed by Celia et al. (1990).

The unsaturated hydraulic properties in HYDRUS–2D are defined by (van Genuchten, 1980; Mualem, 1976)

$$\frac{\theta - \theta_r}{\theta_s - \theta_r} = S_e = [1 + (-\alpha h)^n]^{-m}; \quad m = \frac{n-1}{n} \qquad [12]$$

and

$$K(S_e) = K_s S_e^l \left\{1 - \left[1 - S_e^{(1/m)}\right]^m\right\}^2 \qquad [13]$$

where θ_s is the saturated water content ($L^3\ L^{-3}$); θ_r is the residual water content ($L^3\ L^{-3}$); $\alpha(L^{-1})$, n, and l are curve shape parameters (-); and K_s is the saturated hydraulic conductivity ($L\ T^{-1}$). The simulated flow domain was 3.0 m long (radial direction) by 0.6 m deep, using a grid spacing of 0.05 m in the radial and 0.05 m in the vertical direction.

Boundary and Initial Conditions

For the soil surface boundary conditions, HYDRUS–2D requires estimates of the potential transpiration (T_{pot}) and soil evaporation (E_s). Daily reference evapotranspiration (ET_0) data was provided by a nearby weather station of the California Irrigation Management Information System (CIMIS). Almond potential ET_{alm} was calculated from ET_0 and the appropriate crop coefficients (K_c). Snyder et al. (1988) recommended a value for K_c of 0.91, corresponding to conditions of 60% canopy soil surface coverage for drip-irrigated trees in the Sacramento Valley. Ritchie's (1972) equation was used to estimate soil evaporation. The radiation interception was calculated using the empirical function for maize (*Zea mays* L.) (Snyder et al., 1985), while we used an upper limit of Stage 1 cumulative evaporation of 6 mm and a partitioning factor of 0.4 between Stage 1 and Stage 2 evaporation (Ritchie, 1972). The potential transpiration of almond trees (T_{alm}) was obtained by subtracting E_s from ET (Eq. [9b]). Figure 4 presents the daily boundary conditions as functions of time during the monitoring period that were used for the HYDRUS–2D model simulations.

Due to the lack of flux information, we assumed a unit hydraulic gradient as the lower boundary condition (gravity flow). The calculated two-dimensional soil moisture profile immediately after irrigation, 13 September, was used as initial condition for the numerical simulations.

Parameter Optimization

In addition to the root water uptake parameters z_m, r_m, z^*, r^*, p_z and p_r (Eq. [6]), and the stress response parameter h_{50} (Eq. [8]), the soil hydraulic parameters n and K_s were also optimized. Although the soil hydraulic properties of a nearby location in the same almond orchard were reported by Andreu et al. (1997), the large soil heterogeneity within the orchard made it necessary to also optimize the soil hydraulic parameters simultaneously with the root water uptake model parame-

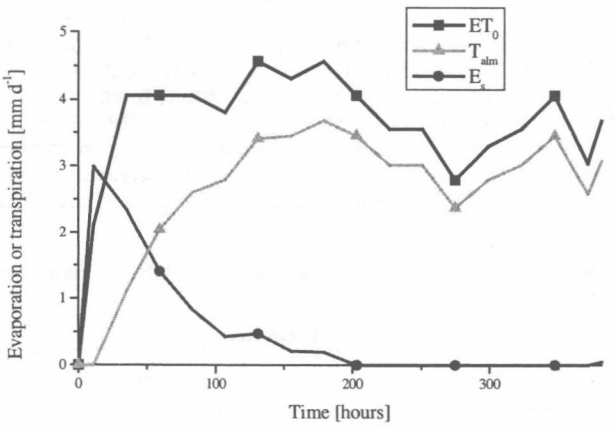

Fig. 4. Soil surface boundary conditions during simulation period (Time 0 corresponds with 13 September).

ters. While fixing the parameters θ_s, θ_r, α, and l to reported values of 0.28, 0.0, 9.4 m^{-1}, and −0.850, respectively (Andreu et al., 1997), spatial variability in soil hydraulic properties was assumed to be characterized by the fitting parameters n and K_s (Eq. [12] and [13]). We fixed the parameters θ_s, θ_r, α, and l to their reported values to partly avoid problems with nonuniqueness of the parameter estimates, especially because a relatively large number of root parameters are already involved in the optimization. Hence, in the calibration stage of this study, a combined total of nine root water uptake and soil hydraulic parameters were optimized simultaneously.

Since optimization algorithms such as Levenberg–Marquardt or Simplex method are only generally applicable to identify a limited number of unique parameters, an alternative was needed to optimize this many parameters. Recently it has been shown that GAs are a powerful tool for parameter identification, when the number of fitted parameters is large (Bäck, 1996; Holland, 1975). Genetic algorithms were developed in evolution theory, based on the concepts of natural selection and genetics. In this approach, variables are represented as genes on a chromosome. Genetic Algorithms feature a group of candidate solutions (population) on a response surface. Through natural selection and using genetic operators, such as mutation and crossover, the objective of a GA is to search for chromosomes with improved fitness, that is, a parameter set, which is closer to the global optimum in the objective function. Natural selection guarantees that chromosomes with the best fitness will propagate in future populations. Using the crossover operator, the GA combines genes from two parent chromosomes to form new chromosomes (children) that have a high probability of having better fitness than their parents. Mutation allows near areas of the response surface to be explored. Hence, GAs offer an improvement in the fitness of the chromosomes through application of the GA in reproduction, so that many generations will create chromosomes containing the optimized variable settings (Wang, 1991).

We applied the GA method presented in Penny and Lindfield (1995), with the small adaptation that the best performing parameter combination is not mutated in the next generation. We used a relatively high crossover value of 0.85 to ensure a relatively fast convergence to the global optimum, where as a mutation factor of 0.15 was used to avoid optimized solutions in local minima. The population size or number of possible first generation parameter combinations was set to 150, whereas the final selected optimized parameter combination was determined after 100 generations. The fitness of a chromosome was calculated by:

$$\mathrm{OF}(b) = \sum_{i=1}^{n} [\theta^*(t_i) - \theta(t_i,\mathbf{b})]^2 \qquad [14]$$

where n is the number of measurements; and $\theta^*(t_i)$ and $\theta(t_i,\mathbf{b})$ denote the measured and predicted water content values, respectively, at time t_i. The parameter vector, **b**, characterizes the chromosome with the genes representing the fitting parameters. The lower the value of objective function, OF(**b**), the more fit is the chromosome. The allowable ranges of the parameters included in **b** are presented in Table 3 and are determined by physical constraints of possible parameter values.

Table 3. Range parameters values used in global optimization with genetic algorithms.

	Parameter								
	z_m	r_m	z^*	r^*	p_z	p_r	h_{50}	n	K_s
	m				(-)		m	-	m d^{-1}
Min	0.00	0.00	0.00	0.00	0.10	0.10	−0.30	1.2	1e-4
Max	0.60	5.00	0.60	5.00	15.0	15.0	−50.0	4.0	0.64

Although GAs are an effective means of determining the global minimum region, their use is not necessarily the most efficient way of finding the exact optimum location. Therefore, the results of the GA were used as initial values for the Simplex optimization to determine the local minimum of Eq. [15] within the global minimum region. Using a sensitivity analysis in which each parameter was varied by 10% around its true value, while keeping the additional parameters fixed at their value found by the GA, we selected those six parameters in the parameter vector that were most sensitive to the model output. Both the GAs and the simplex optimization were carried out using MATLAB, version 5.3 (The Mathworks, 1999). The estimated standard deviation of each parameter b_j of **b** was determined from the diagonal elements of the parameter covariance matrix C (Kool and Parker, 1988),

$$s_j = \sqrt{C_{jj}} \qquad [15]$$

whereas final fitting results were expressed as RMSE values, computed from

$$\mathrm{RMSE} = \sqrt{\frac{\sum_{i=1}^{n} [\theta^*(t_i) - \theta(t_i,\mathbf{b})]^2}{n - m}} \qquad [16]$$

where m is the total number of parameters.

RESULTS AND DISCUSSION

Final parameter values after performing the GA and the Simplex optimization are presented in Table 4. This table also includes final derived parameter values, such as z^{max}, r^{max}, and the 95% confidence intervals using the residuals and Jacobian matrix at the final solution. The fitting results are expressed by RMSE values. As the parameters z_m, r_m, z^*, r^*, n, and K_s showed the highest sensitivity to the model output in the parameter solution obtained with the GA, these six parameters were further optimized using the SA. Because of the simultaneous fitting of this many parameters, problems may occur with the nonuniqueness of the parameter estimates

Table 4. Optimized parameter values after genetic algorithm (GA) and Simplex algorithm (SA). Also included are the 95% parameter confidence intervals of the final solution and the coefficient of variation of the final parameter estimates.

				95% Confidence interval		
Parameter		GA	SA	Lower	Upper	CV
						%
z_{zm}	(m)	0.426	0.403	0.326	0.481	9.6
r_m	(m)	4.174	4.144	3.463	4.825	8.3
p_z	(-)	3.214	†	2.319	4.109	13.9
p_r	(-)	2.918	†	2.412	3.424	8.7
z^*	(m)	0.300	0.330	0.189	0.469	21.2
r^*	(m)	2.052	2.075	1.862	2.288	5.1
n	(-)	1.673	1.674	1.545	1.803	3.9
K_s	(cm d^{-1})	0.408	0.460	0.350	0.569	11.9
h_{50}	(m)	−0.533	†	−0.733	−0.333	18.7
RMSE	(m^3 m^{-3})	0.0157	0.0154			
R^2		0.91	0.92			
Derived Parameters						
z^{max}	(m)	0.294	0.278			
r^{max}	(m)	2.053	2.075			

† Open space indicates that parameter was held constant at value estimated by GA.

caused by the presence of multiple local minima in the objective function.

Since parameter estimation involves a variety of possible errors, including measurement, model and numerical errors, an uncertainty analysis of the optimized parameters constitutes an important part of parameter estimation. Table 4 shows that the standard deviations of the various parameters are typically small, revealing that the information of the water content measurements for most of the parameters is robust (e.g., Vrugt et al., 2001). Although a variety of errors determine the final parameter standard deviation, the root parameters p_z and z^*, have a relatively higher uncertainty as compared to the other root parameters. Their larger values of the coefficient of variation (CV), may be caused by the smaller number of nodal points defining a strip in the depth direction as compared to the radial direction. Furthermore, the 95% confidence interval of the n-parameter in the soil hydraulic functions lies within the range of n-values between 1.44 and 1.99 as reported by Andreu et al. (1997) at a nearby location between the 0- and 60-cm depth. The relatively high uncertainty in h_{50} as indicated by its CV value, is partly because of its extreme large value, corresponding with a low water holding capacity of this soil. Although not presented, inspection of the parameter correlation matrix for the final solution showed that correlations between the parameter estimates are typically low ($R < 0.50$), except between parameter r_m and z^* ($R = -0.88$), r_m and r^* (R = 0.92), z^* and r^* ($R = 0.88$), and n with K_s (0.88).

The optimized soil water retention and unsaturated soil hydraulic conductivity curves from the final SA solution are presented in Figure 5. Also included are the measured (θ,h) data using the multistep outflow method from soil cores taken at a 30-cm depth at a nearby location, and (K,θ) points as obtained using the instantaneous profile method at a nearby location at the 30-cm soil depth (Andreu et al., 1997). Both the measured (θ,h) points and the optimized retention curve clearly show the small water holding capacity of this shallow gravely soil. Additionally, the optimized unsaturated hydraulic conductivity and measured (K,θ) points show the rapid decrease of the hydraulic conductivity with decreasing water content. Moreover, the large soil water stress value ($h_{50} = -0.53$ m) is in agreement with the low water holding capacity of this soil. The optimized saturated conductivity of 0.46 cm d^{-1} of the SA optimization is much lower than the reported range of 34.1 to 62.4 cm d^{-1} between 0- and 60-cm depth by Andreu et al., 1997. However, one should realize that the saturated hydraulic conductivity in this study, is much more a water balance parameter controlling the magnitude of the lower boundary flux than it is a soil physical parameter affecting soil water flow in the soil domain.

The range of the maximum rooting depth (z_m) as found by the SA (0.33 m $< z_m <$ 0.48 m) is in excellent agreement with the results obtained by Koumanov et al. (1997) for the same experimental plot, suggesting that active root water uptake was limited to the top 40 cm only using seasonal root and soil water content

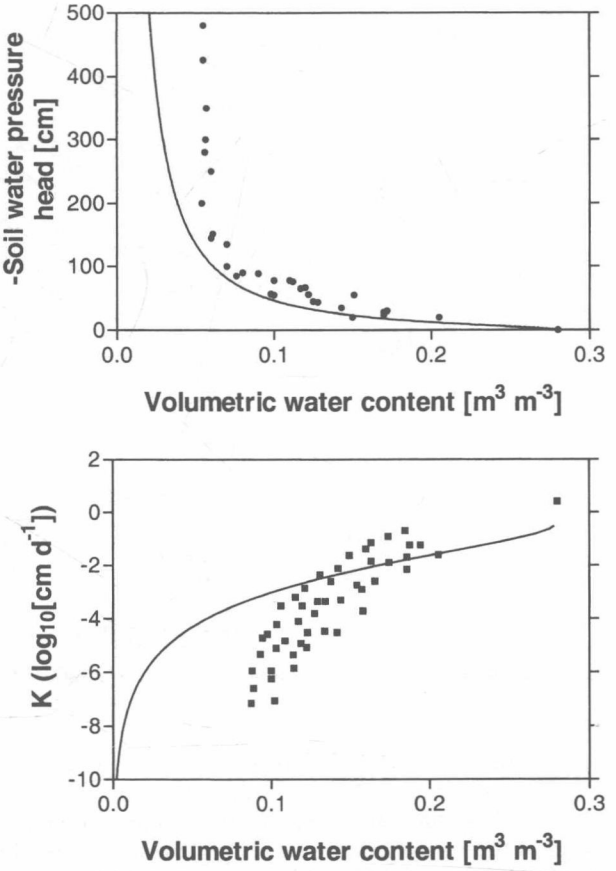

Fig. 5. Optimized soil water retention and unsaturated hydraulic conductivity curves as obtained by the Simplex Algorithm optimization and measured (θ,h) using the multistep outflow method from soil cores taken at 30-cm depth at a nearby location and (K,θ) points, as obtained using the instantaneous profile method at a nearby location for the 30-cm soil depth.

observations.Whereas our optimization results indicate the depth of maximum root water uptake is about 0.28 m, the study by Andreu et al. (1997) concluded that maximum uptake occurred at the soil surface (0–15 cm) and decreased further down the soil profile. However, their study did not include soil evaporation as a possible mechanism of soil water depletion near the soil surface. The optimized radial position of maximum root water uptake (r^{max}) of the almond tree (2.07 m) agreed well with the region of highest irrigation application amounts of the microsprinkler (Koumanov et al., 1997). This was so, despite the location of the microsprinkler at the far corner along the tree row (see Fig. 3), and was caused by systematic nonuniform water applications during the irrigation period. This finding is consistent with the experimental data of Coelho and Or (1996), who concluded that the applied irrigation strategy can determine root development in both space and time.

Figure 6 presents the optimized spatially distributed root water uptake model, $\beta(r,z)$, as determined over the 16-d monitoring period using the final optimized root water uptake parameters. Clearly, the zone of maximum root water uptake is concentrated in a thin soil layer between 0.1 and 0.35 m. In this area, the roots act like a sink and provide for soil water potential differ-